Submitted to Astroparticle Physics

astro-ph/9602045
INFNFE-01-96
INFNCA-TH9601

arXiv:astro-ph/9602045v1 9 Feb 1996

Physics potentials of pp and pep solar neutrino fluxes

E. Calabresu,[1] G. Fiorentini,[2] and M. Lissia[1]
[1] *Istituto Nazionale di Fisica Nucleare, via Ada Negri 18, I-09127 Cagliari, Italy; and Dipartimento di Fisica dell'Università di Cagliari, I-09124 Cagliari, Italy*
[2] *Dipartimento di Fisica dell'Università di Ferrara, I-44100 Ferrara, Italy; and Istituto Nazionale di Fisica Nucleare, Sezione di Ferrara, I-44100 Ferrara, Italy*
(January 1996)

Abstract

Experimental determinations of the *pp* and *pep* fluxes have great potentialities. We briefly review the reasons that make such measurements privileged tests of neutrino properties. We discuss the predictions for these fluxes given by four *good* solutions to the solar neutrino problem: small- and large-angle MSW and Just-So oscillations into active neutrinos, and small-angle MSW oscillations into sterile neutrinos. In addition, we examine the impact of the planned Hellaz detector, which should measure separately the ν_e and ν_μ fluxes in the *pp* energy window and the signal from the *pep* neutrinos, for distinguishing among the different solutions and for determining the solar central temperature.

Typeset using REVTEX

A. Introduction

Theoretical understanding of stellar structure has reached a rather mature stage and can be confronted with refined experimental tests in a wide range of conditions. In particular, present solar models accurately reproduce even the very detailed experimental information coming from helioseismology. Therefore, we are nowadays quite confident in the predictions of standard solar models (SSMs) for the main neutrino fluxes, especially *pp*, *pep* and ^{7}Be neutrinos [1–5]. Nevertheless, all the present experimental determinations of solar neutrino fluxes are at odds with the theoretical predictions, strongly suggesting that neutrinos might have nonstandard properties [6–8].

In this context, direct measurements of the *pp* and *pep* neutrino fluxes would be of the outmost importance. Predictions for these fluxes are the most robust and the least dependent on the detail of the solar models so that comparison with experiment could provide a powerful test of the different nonstandard-neutrino solutions. Moreover, future experiments, e.g. Hellaz [9], aimed to measure both the ν_e and ν_μ flux would further increase the relevance of such a test. The significance of a measurement of the other main solar neutrino flux (^{7}Be) has been discussed previously [8,10,11].

Therefore, this paper aims to three main objectives:

- to summarize what is known about the production of *pp* and *pep* neutrinos in the Sun;
- to examine predictions of different particle physics solutions to the solar neutrino problem (SNP) for the fluxes and spectra of *pp* and *pep* neutrinos at the Earth surface;
- to discuss the physics potential of a planned detector of *pp* and *pep* neutrinos (Hellaz) for distinguishing among the possible solutions and for measuring the central temperature of the Sun.

B. pp and pep neutrinos from the Sun

The *pp*-neutrino production rate from the Sun, L_{pp}, is predicted quite accurately; for example the last SSM of Bahcall and Pinsonneault [5] (BP95) yields:

$$L_{pp}^{SSM} = 1.66 \cdot (1 \pm 0.01) \cdot 10^{38}\,\mathrm{s}^{-1}\,. \tag{1}$$

If neutrino are standard, i.e. electron neutrinos do not decay nor are converted to other flavors, this production rate determines the flux of *pp* neutrinos on Earth at the distance R_{TS} of one astronomical unit:

$$\Phi_{pp}^{SSM} = 5.91 \cdot (1 \pm 0.01) \cdot 10^{10}\,\mathrm{cm}^{-2}\mathrm{s}^{-1}\,. \tag{2}$$

There is no surprise for such a small uncertainty, since the *pp*-neutrino production is strongly correlated with solar energy production, which is fixed by the presently observed luminosity. Actually, very simple considerations set an extremely reliable upper bound to L_{pp}, which turns out to be close to the SSM estimate. The maximum production rate L_{pp}^{max} clearly corresponds to the case that only *pp* neutrinos are emitted from the Sun. Given the *pp*-neutrinos average energy $\langle E \rangle_{pp} = 0.265$ MeV, the total energy released per fusion $Q =$

26.73 MeV and the observed solar luminosity [5] $L_\odot = 2.399 \cdot (1 \pm 0.0042) \cdot 10^{39}\,\mathrm{MeV\ s^{-1}}$, one finds:

$$L_{pp}^{max} = L_\odot/(Q/2 - \langle E \rangle_{pp}) = 1.831 \cdot (1 \pm 0.004) \cdot 10^{38}\,\mathrm{s^{-1}}\,. \tag{3}$$

Correspondingly, the maximal *pp* flux on Earth is:

$$\Phi_{pp}^{max} = 6.512 \cdot (1 \pm 0.004) \cdot 10^{10}\,\mathrm{cm^{-2} s^{-1}}\,. \tag{4}$$

The reason that Φ_{pp}^{SSM} is so close to this number is that SSM predicts that more that 90% of the total number of neutrinos are *pp* neutrinos.

Nonstandard solar models differ from the SSM and among themselves because they have different physical inputs. Most of the effect of changing some of these inputs is reasonably well parameterized by a single parameter: the central temperature T [12,13]. For the sake of simplicity and concreteness, we shall often talk of changing the (central) temperature T without referring to the specific way this change is obtained.

When the temperature changes, the relative efficiencies of the different chains (*pp*-I, *pp*-II, *pp*-III and CNO) also change, but the total neutrino production rate remains practically constant, since its value is strongly constrained by the luminosity. As an example, if T increases with respect to T^{SSM}, the *pp*-II chain becomes more efficient and yields a larger production of ^{7}Be neutrinos; the CNO efficiency and neutrinos also increase. Correspondingly, the *pp* production decreases, even if its dependence on the temperature is rather weak. By using a parameterization of the form:

$$L_{pp} = L_{pp}^{SSM} \left(\frac{T^{SSM}}{T} \right)^{\beta_{pp}}\,, \tag{5}$$

the parameter β_{pp} ranges from 0.6 to 0.85 depending on how the temperature change is achieved [13,14].

This dependence implies that even a 5% variation of T, which is a really huge variation on the scale of the SSM uncertainties ($\Delta T \approx 1\%$), changes L_{pp} by just a few percent.

The *pep* neutrinos are estimated to be a tiny fraction of *pp* neutrinos. Their ratio

$$\xi \equiv L_{pep}/L_{pp} \tag{6}$$

is just $\xi = 2.37 \cdot 10^{-3}$ in the SSM of BP. The corresponding flux on Earth, if all neutrinos survive, is $\Phi_{pep}^{SSM} = 1.40 \cdot 10^8\,\mathrm{cm^{-2} s^{-1}}$.

The value of ξ is rather stable among the different SSM calculations (all SSMs give the same value of ξ within about 10%) and it is also weakly sensitive to the central solar temperature. By writing

$$\frac{\xi}{\xi^{SSM}} = \left(\frac{T}{T^{SSM}} \right)^{\beta_\xi}\,, \tag{7}$$

the parameter β_ξ takes values in the range from -1.6 to 2.8, depending on the parameter which is varied to tune the central temperature [13,14].

The uncertainty on ξ is at most 15% for a 5% variation of temperature, and again this should be taken as an extreme possibility for SSMs.

Concerning the energy distribution, kinematics fixes the energy of monochromatic *pep* neutrinos ($E_{pep} = 1.442$ MeV) and nuclear physics determines the shape of the *pp* spectrum, essentially through phase space considerations; this latter spectrum is shown in Fig. 1 (solid curve).

We remind that SSMs give also a very robust (stable) prediction for the flux of ^{7}Be neutrinos. Nevertheless, the accuracy quoted for this flux is lower than the one for the *pp* and *pep* fluxes:

$$\Phi_{Be}^{SSM} = 5.15 \cdot (1 \pm 0.06) \cdot 10^9 \, \mathrm{cm}^{-2}\mathrm{s}^{-1} \, . \tag{8}$$

This fact is also reflected in its somewhat stronger temperature dependence:

$$\frac{\Phi_{Be}}{\Phi_{Be}^{SSM}} = \left(\frac{T}{T^{SSM}} \right)^{\beta_{Be}} \, , \tag{9}$$

where now β_{Be} goes from about 8.7 to about 11.5.

All in all, theoretical predictions for the number of *pp* and *pep* neutrinos emitted per second from the Sun look quite reliable and stable, and require really a minimum of solar physics, essentially energy conservation.

C. The pp and pep neutrinos on Earth

Among the several particle physics solutions to the SNP, mechanisms where ν_e oscillate into neutrinos of other flavors (for the sake of definiteness ν_μ) or into sterile neutrinos (ν_s) are particularly appealing, as they require very little adjustment of the minimal electro-weak standard model.

In particular, matter enhanced (MSW) oscillations and "Just-So" oscillations give a simple and satisfactory description of the data [15–19,11].

In this context the available experimental results support only four specific solutions [8], which are reported in Table I. Oscillations into active neutrinos provide good fits to the data in the mass range relevant to the MSW mechanism both at small and large mixing-angle, and also in the mass range relevant to Just-So oscillations. Oscillations into sterile neutrinos give instead a good fit to the data only within the MSW small-mixing-angle solution.

The predicted fluxes of ν_e and ν_μ in the *pep* and *pp* energy regions (these latter integrated over their energy spectrum) at the best fit points are also shown in Table I, whereas Figs. 2 and 3 show the ranges of Φ^μ predicted at the 90% CL by the four acceptable models.

Concerning *pp* neutrinos (see Fig. 2), the MSW small-mixing-angle solution predicts a very low (strictly null if neutrinos are sterile) ν_μ signal: the ν_e flux is little or not at all suppressed both in the case of active and sterile neutrinos. In fact, it is well-known that MSW small-mixing-angle solutions of the SNP are characterized by a strong suppression of the ν_e flux only in a small energy window centered at intermediate energies. Therefore, the study of solar neutrinos in the *pp* energy range cannot distinguish these solutions from the case of standard neutrinos. On the other hand, the Just-So and MSW large-mixing-angle solutions predict a ν_μ (ν_e) flux on Earth about 40% (60%) of the SSM estimate.

The situation looks significantly different for *pep* neutrinos (see Fig. 3). The MSW small-angle cases predict a *pep* ν_e flux that is essentially vanishing, since the *pep* energy falls within

the suppression window. Therefore, this solution gives a ν_μ flux that is about equal to the *pep* SSM flux, if neutrinos are active. The MSW large-angle solution gives again a ν_μ flux about one half of the SSM one. On the other hand, the Just-So model can accommodate almost any value of the *pep* ν_μ (ν_e) flux. In this respect, it is worth observing that a ν_μ flux close to zero (unsuppressed ν_e flux) is only acceptable in the context of Just-So oscillations or sterile neutrinos.

Thus a simultaneous measurement of the ν_μ (or ν_e) flux for both *pep* and *pp* neutrinos has a remarkable discriminating power among the various solutions, as it is clearly shown in Fig. 4 where we present the expected (Φ^μ_{pp},Φ^μ_{pep}), normalized to the SSM predictions. In particular, note that the MSW small-angle solution for active neutrinos, which cannot be distinguished from standard neutrinos when looking just at the *pp* energy range, yields drastically different predictions for the *pep* neutrinos. In addition, large parts of the 90% CL regions predicted by MSW large-angle and Just-So oscillations uniquely characterize one of the two solutions, even if there is some ambiguity when Φ^μ_{pp} is about 40% of Φ^{SSM}_{pp} and Φ^μ_{pep} between 50% and 80% of Φ^{SSM}_{pep}. However, the distinguishing of sterile from standard neutrinos needs independent information on the ν_e flux.

A more complete picture of the possible outcomes and implications of an experiment capable of measuring both Φ_e and Φ_μ is shown in Figs. 5 and 6, which we are going to discuss in detail, for the *pp* and *pep* neutrinos, respectively.

If we assume that ν_e transform into ν_μ and/or ν_s, the fluxes on Earth satisfy:

$$\Phi^e_{pp} + \Phi^\mu_{pp} + \Phi^s_{pp} = \frac{L_{pp}}{4\pi\, R^2_{TS}}\,. \tag{10}$$

We have already seen in the previous section that solar energetics provides an upper bound to L_{pp} and, consequently, there exists an upper bound on the sum of electron and muon neutrinos:

$$\Phi^e_{pp} + \Phi^\mu_{pp} \leq \Phi^{max}_{pp}\,; \tag{11}$$

this upper bound is shown as a dashed line in Fig. 5. Thus, whatever be the mechanism responsible for the solar neutrino problem and independently of the SSM, experimental findings should stay below this line.

If one relies on the SSM prediction for the *pp* flux Φ^{SSM}_{pp}, one has instead:

$$\Phi^e_{pp} + \Phi^\mu_{pp} \leq \Phi^{SSM}_{pp}\,. \tag{12}$$

In Fig. 5, this SSM bound is represented by the shaded band; the width of this band indicates the uncertainty of the SSM *pp* flux. This figure shows clearly that the SSM bound is not much lower than the more general bound coming from the luminosity constraint, Eq. (11), in accordance with the well-known fact that most of total energy of SSM comes from the *pp*-I chain.

The equal sign in Eqs. (11) and (12) only holds in the absence of sterile neutrinos, so that a measurement yielding Φ^e_{pp} and Φ^μ_{pp} along this line would be a clear indication against sterile neutrinos.

Should instead the experiment give a point below this line, this result would imply either conversion into sterile neutrinos or a solar central temperature significantly higher than the one estimated by the SSM (we recall that as temperature increases Φ_{pp} decreases).

The predictions of the four candidate solutions (best points and 90% CL regions) are also shown in Fig. 5. While the sterile neutrino solution lays on the horizontal axis, all three active neutrino solutions lay along the shaded band that represents the SSM prediction. The dashed arrow indicates the limit of the 90% intervals on the band or on the horizontal axis.

Similar considerations can be applied to *pep* neutrinos, see Fig. 6. We remark that the study of *pep* neutrinos can clearly discriminate between oscillations into active and sterile neutrinos for the MSW small-angle solution (see Fig. 6), whereas the corresponding predictions for the *pp* neutrinos are not so clearly separated (see Fig. 5). In addition, the study of *pep* neutrinos is able to discriminate between Just-So and MSW large-angle solution for a significant portion of the possible outcomes (compare the 90% intervals predicted by these two solutions in Fig. 5 with the corresponding intervals in Fig. 6).

In principle, measurements of the *pp* neutrino energy spectrum could provide additional information and help discriminating the different solutions. The *pp* ν_e energy spectra predicted by the different schemes are shown in Fig. 1 together with the one given by the SSM. Deformations of the spectrum are tiny for the MSW solutions, and the only effect is basically a change of the normalization of the flux. On the contrary, Just-So oscillations predict in principle a strong energy dependence for the yearly averaged signal in the *pp* region (solid oscillating line in Fig. 1). The spectral deformation is even more clear in Fig. 7 (a) where we plot the ratio of the ν_e flux to the SSM prediction as function of energy. In practice, however, a low energy resolution can miss this strongly oscillating energy deformation. The histograms (b), (c) and (d) in Fig. 7 have been made with bins of size $\Delta E =$ (a) 10, (b) 20 and (c) 50 keV to estimate the necessary energy resolution. While a bin size of 20 keV is still capable to resolve the energy dependence, a bin size of 50 keV seems insufficient to this purpose.

For the Just-So case, we have the additional possibility of seasonal modulations, since the oscillation length is comparable to the Sun-Earth distance. Detection of this effect would be a distinctive indication of the Just-So mechanism.

However, when looking at *pp* ν_e, a 50 keV energy bin is sufficient to average out the phase of the modulation (see Fig. 7) and, therefore, completely suppresses these seasonal modulations, since it is the same phase $\phi \sim \Delta m^2 * R/E$ that controls spatial (R) and energy (E) oscillations. The possibility of seeing these modulations in the *pp* energy spectrum would require high statistics in small energy bins (about 10 keV). But, if such resolution and statistics were available, the energy dependence of the signal would give a much better indication of Just-So oscillation than the seasonal variation, since the energy spectrum can cover several wave lengths ($\Delta\phi \gg \pi$), while the change of the Earth-Sun distance corresponds to only a fraction of the wave length ($\Delta\phi \leq \pi/4$ at $E = 300$ keV).

In this respect, the monoenergetic *pep* neutrinos are more interesting. Semiannual modulations as large as $\pm 35\%$ of the average ν_e flux are possible, as it is exemplified by the dashed curve in Fig. 8. It is worth remarking that these modulations are large when the suppression is about 50% (as natural since the derivative respect to the oscillation wavelength, and then to the energy, is maximal), which is the case when this additional information is the most valuable, since the yearly averaged information cannot discriminate between Just-So and

MSW large-angle solutions, see Figs. 2 and 3. On the contrary, the seasonal variation is minimal when the *pep* signal is either maximal or minimal, as it happens at the best fit point, but in this case the yearly average signal is sufficient for discriminating among the solutions.

D. The potential of the Hellaz experiment

The proposed Hellaz detector [9] aims at measuring both the ν_e and ν_μ fluxes in the *pp* energy region, Φ^e_{pp} and Φ^μ_{pp}, by exploiting the different angular dependence of the ν_e and ν_μ scattering cross section on electrons. These two fluxes should be separately determined. The expected statistics should allow measurements in at least four energy bins. The energy bins reported in the present proposal [9] are shown in Table II, where we also show the predicted events according to the SSM. Note, however, that the energy resolution of the single events is expected to be higher, about 9–24 keV at $E = 300$ keV, than the width of these bins.

For higher energy (*pep* and ^{7}Be) neutrinos, the difference between ν_e and ν_μ cross sections becomes less pronounced and flavor discrimination is not possible. Then the experiment determines just the following combination of fluxes:

$$\Phi^H_{pep,Be} = \Phi^e_i + \alpha_i \Phi^\mu_i \qquad (i = pep,\, Be)\,, \tag{13}$$

where α is the ratio of neutral current (NC) to NC plus charged current (CC) cross sections at the *pep* or ^{7}Be neutrino energy (1.442 MeV and 0.861 MeV, respectively). Approximately, these ratios are:

$$\alpha_{pep} = 1/5 \tag{14}$$

$$\alpha_{Be} = 1/4\,. \tag{15}$$

1. What can Hellaz tell us about neutrino oscillations?

Part of the physics potential of Hellaz is indicated in the last three rows of Table I, where we present Φ^e_{pp}, Φ^μ_{pp} and the *pep* signal S_{pep} at the best fit points for each solution.

Of course, the muon signal is a privileged indicator of neutrino oscillations; note, however, that — as already remarked — the MSW small-angle solutions, for either sterile or active neutrinos, predict small or even vanishing muon signals in the *pp* energy region. In other words, these solutions look very much the same as if neutrinos were standard from the point of view of *pp* neutrinos. In this case, a simultaneous measurement of the *pep* signal is particularly important, since it should clearly discriminate MSW small-angle solutions from standard neutrinos.

The capability of discriminating among the various solutions is thus best understood from Fig. 9, where we present the correlation among the *pep* signal S_{pep} and the muon flux in the *pp* energy region Φ^μ_{pp}. This figure is essentially similar in spirit to Fig. 4, but it involves quantities that should be directly measured by Hellaz. This combined measurement should unambiguously discriminate the two MSW small-angle solutions from the others (and from

each other). If the actual solution is the Just-So mechanism, this combined measurement can distinguish it from the MSW large-angle solution only if the *pep* signal is close to its SSM prediction, as it happens at the best fit point, or close to maximal suppression.

We remark that the study of the yearly averaged and energy integrated signals cannot essentially distinguish between the Just-So and MSW large-angle mechanisms, at least for part of the possible values of parameters Δm^2 and θ within their 90% CL regions, those values that yield a *pep* signal between 40% and 70% the SSM signal. As previously noted, however, these ambiguous cases might be discriminated by the detection of the semiannual modulations that are foreseen for the signal of the monochromatic neutrino lines. The time dependence of the survival probability $\Phi^e_{pep}/\Phi^{SSM}_{pep}$ (solid line) and of the corresponding signal S_{pep}/S^{SSM}_{pep} (dashed line) expected at the point of maximal variation (dashed line) are shown in Fig. 8, as a characteristic example. We remind that the variation is maximal when the average signal is most ambiguous, i.e. about a half of the SSM value, and in this case a few hundred events should be sufficient for a 3σ evidence. We verified that 1000 SSM events should allow a 3σ detection of seasonal variations predicted by parameters in almost the whole 90% confidence region of the Just-So solution. This number of SSM events could be reached in a little more than one year of operation if HELLAZ is filled with CF_4 gas as it has been proposed specifically to detect these higher-energy neutrinos [20]. Only when S_{pep} is close to its maximum or minimum this statistics is not sufficient.

In addition, one can exploit the information coming from the energy dependence of the signal (spectral deformation).

As anticipated in the general discussion in the previous sections, we do not expect a large spectral deformation corresponding to the three MSW candidate solutions. In Table II, we show the calculated ν_e flux, averaged in each energy bin and normalized to the same quantity in the SSM, at the best fit points of each solution. Variations among the different bins are just a few per cent, which are comparable to the expected statistical fluctuations.

However, it is possible to find values of the parameters (Δm^2 and θ) within the 90% CL region of the MSW small-angle solution (not the values at the best fit as we see in Table II) such that there is some detectable suppression, even at the level of 30%, of Φ^e in the highest energy bin relative to the others. The physical explanation is that the suppression window (which is a function of $\Delta m^2/E$) for sufficiently small neutrino masses can reach the upper part of the *pp* energy spectrum. The detection of such a deformation would provide a specific signature of this type of solutions, while not seeing such deformation would further reduce the 90% CL region of the MSW small-angle solution.

For the Just-So candidate solution a large spectral deformation is expected. Energy resolution is crucial in this case (see Fig. 7). More specifically, an energy resolution between 9 and 24 keV for single events, which should be obtained by Hellaz, should be able to detect such deformation given the expected statistics [20]. On the contrary, most of the structure is washed out by 50 keV energy bins.

We can summarize this last point saying that Hellaz should be capable of performing accurate solar neutrino spectroscopy in the extremely important low energy range and that there are concrete possibilities that in this energy range there could be a detectable spectral deformation.

2. What can Hellaz teach us about the Sun?

Apart from the problem of neutrino oscillations, detection of *pp* and *pep* neutrinos could also be very interesting for studying properties of the solar interior, and in this respect we would like to add the following comments.

Ignoring for the moment the possibility of conversion into sterile neutrinos, a measurement of Φ^e_{pp} and Φ^μ_{pp} provides a measurement of the solar central temperature T, since:

$$\Phi^e_{pp} + \Phi^\mu_{pp} = \Phi^{SSM}_{pp} \left(\frac{T^{SSM}}{T} \right)^{\beta_{pp}} . \tag{16}$$

where $\beta_{pp} \approx 0.7$.

Hellaz, which should be able to determine the total flux within 15%, could measure the solar temperature with a 20% uncertainty. This uncertainty is much larger than the estimated theoretical one. Nevertheless, direct temperature determination of the solar interior looks fascinating.

In principle, the ^{7}Be neutrinos could be more precise indicators of the solar temperature, since the corresponding β coefficient is higher:

$$8.7 \leq \beta_{Be} \leq 11.5 \, . \tag{17}$$

A determination of these fluxes with 10% accuracy would give the temperature at the 1% level. In the present proposal of Hellaz [9] separate determinations of Φ^e_{pep} and Φ^μ_{pep} are not foreseen, but it is nevertheless interesting to keep in mind such a possibility.

These statements hold ignoring the possibility of sterile neutrinos. Note however that all our favorite solutions do not predict any sterile neutrinos in the *pp* energy range (at least if one excludes the Hellaz highest energy bin). More generally, if one includes the possibility of sterile neutrinos, the above-derived values of T should be interpreted as upper values on the true solar central temperature.

E. Conclusions

Theoretical predictions for the production rate of *pp* and *pep* neutrinos in the Sun require little knowledge of solar physics, basically energy conservation, and, therefore, are quite reliable and stable. Expectations for the ν_μ flux at *pp* and *pep* energies are summarized in Figs. 2 and 3, respectively, for different solutions to the solar neutrino problem. We remark the following points:

(1) The combined measurement of both pp and pep neutrinos is extremely discriminating among the various solutions, see Fig. 4 and 9.

(2) Deformations of the *pp* energy spectrum, particularly those predicted by the Just-So mechanism (Fig. 7), should be observable in detectors with the energy resolution such as that claimed by Hellaz (9–24 KeV) [9,20].

(3) Seasonal variations of the *pep* signal, as predicted by the Just-So mechanism (Fig. 8), should also be detected by Hellaz, once it is filled with CF_4 to increase the statistics of these higher-energy neutrinos.

ACKNOWLEDGMENTS

It is our pleasure to thank T. Ypsilantis for several fruitful and informative discussions and for a critical reading of the manuscript.

After the completion of this paper we received a preprint by J. N. Bahcall and P. I. Krastev [21] that contains material that partially overlaps with the one discussed in present work.

REFERENCES

[1] J. N. Bahcall and R. Ulrich, Rev. Mod. Phys. 60 (1988) 297.

[2] J. N. Bahcall, *Neutrino Astrophysics* (Cambridge University Press, Cambridge, England, 1989).

[3] J. N. Bahcall and M. H. Pinsonneault, Rev. Mod. Phys. 64 (1992) 885.

[4] S. Turck-Chièze et al., Phys. Rep. 230 (1993) 57.

[5] J. N. Bahcall and M. H. Pinsonneault, Rev. Mod. Phys. 67 (1995) 1.

[6] V. Berezinsky, Comments Nucl. Part. Phys 21 (1994) 249.

[7] V. Berezinsky, LNGS Preprint 95/60 (1995).

[8] E. Calabresu, G. Fiorentini, M. Lissia and B. Ricci, physics e-print hep-ph/9511286, to appear in Nucl. Phys. B (Proc. Suppl.) (1996).

[9] J. Seguinot, T. Ypsilantis, G. Bonvicini, P. Giusti, G. Laurenti and A. Zichichi, College de France preprint LPC/95-08 (1995).

[10] S. Degl'Innocenti, G. Fiorentini and M. Lissia, physics e-print hep-ph/9408386, published in Nucl. Phys. B (Proc. Suppl.) 43 (1995) 66.

[11] E. Calabresu, N. Ferrari, G. Fiorentini and M. Lissia, physics e-print archive hep-ph/9507352, published in Astropart. Phys. 4 (1995) 159.

[12] N. Hata and P. Langacker, Phys. Rev. D 50 (1994) 632.

[13] V. Castellani et al., Phys. Rev. D 50 (1994) 4749.

[14] J. N. Bahcall and A. Ulmer, physics e-print archive astro-ph/9602012, to appear in Phys. Rev. D.

[15] S. L. Glashow and L. M. Krauss, Phys. Lett. B 190 (1988) 199.

[16] V. Barger, R. J. N. Phillips and K. Whisnant, Phys. Rev. Lett. 69 (1992) 3135.

[17] S. T. Petcov, Nucl. Phys. B (Proc. Suppl.) 43 (1995) 12; P. I. Krastev and S. T. Petcov, physics e-Print archive hep-ph/9510367 (1995); and references therein.

[18] N. Hata and P. Langacker, e-Print archive hep-ph/9308252 (1993);
N. Hata, e-Print archive hep-ph/9402311 (1994).

[19] Z. G. Berezhiani and A. Rossi, Phys. Rev. D 51 (1994) 5229;
Z. G. Berezhiani and A. Rossi, physics e-Print archive hep-ph/9507393 (1995).

[20] T. Ypsilantis, private communication.

[21] J. N. Bahcall and P. I. Krastev, physics e-Print archive hep-ph/9512378, to appear in Phys. Rev. D (1996).

TABLES

TABLE I. Predictions for *pep* and pp neutrinos. For four different solutions we present, at the best fit point (Δm^2, $\sin^2 2\theta$), the χ^2 per degree of freedom, the fluxes of ν_e and ν_μ originating from *pep* and *pp* reaction in units of SSM fluxes. For *pep* neutrinos we also present the fraction of the SSM signal predicted for a CC+NC detector.

	active			sterile
	MSW small θ	MSW large θ	Just So	MSW small θ
Δm^2 [eV^2]	$7.9 \cdot 10^{-6}$	$1.7 \cdot 10^{-5}$	$6.0 \cdot 10^{-11}$	$4.9 \cdot 10^{-6}$
$\sin^2 2\theta$	$5.8 \cdot 10^{-3}$	0.63	1.00	$7.9 \cdot 10^{-3}$
$\chi^2/d.o.f.$ [a]	0.9/2	1.5/2	1.9/2	0.7/2
$\Phi^e_{pep}/\Phi^{SSM}_{pep}$	0.056	0.408	0.013	0.017
$\Phi^\mu_{pep}/\Phi^{SSM}_{pep}$	0.944	0.592	0.987	0.983
$\Phi^e_{pp}/\Phi^{SSM}_{pp}$	0.986	0.643	0.508	0.979
$\Phi^\mu_{pp}/\Phi^{SSM}_{pp}$	0.014	0.357	0.492	0.021
S_{pep}/S^{SSM}_{pep}	0.245	0.526	0.211	0.017

[a]For comparison standard neutrinos yield $\chi^2/d.o.f. = 904.1/4$.

TABLE II. The first column shows the number of events expected in the Hellaz detector after one year of operation [9] for standard neutrinos and SSM. The next four columns show the ν_e survival probability according to the four solutions of Table I. The first five rows report results for the indicated energy bins in the pp energy region and the last two rows for the ^{7}Be and *pep* lines.

	number of events for standard ν	Φ^e/Φ^{SSM}			
		active			sterile
		MSW small θ	MSW large θ	Just So	MSW small θ
energy bins [keV]					
220–270	349	0.99	0.66	0.49	0.99
270–320	634	0.99	0.65	0.49	0.99
320–370	840	0.98	0.64	0.56	0.98
370–420	620	0.98	0.63	0.47	0.96
220–420	2443	0.99	0.65	0.51	0.98
lines ([MeV])					
^{7}Be (0.861)	1500	0.09	0.48	0.78	0.02
pep (1.442)	100 [a]	0.06	0.41	0.01	0.02

[a]For these more energetic neutrinos, it has been proposed to fill HELLAZ with CF_4, which would give about 850 events per year.

FIGURES

FIG. 1. The yearly averaged ν_e spectrum on Earth in the *pp* energy region ($0 < E < 440$ keV) for SSM (smooth solid line), MSW global best fit point in the small-θ region (dotted line), MSW local best fit point in the large-θ region (dashed line) and Just-So best fit (oscillating solid line). The spectrum of the small-θ solution for sterile neutrinos is not distinguishable from the one for active neutrinos (dotted line). For graphical reasons, the ν_e spectrum predicted by the Just-So best fit has been averaged below 150 keV eliminating the oscillation, which has an amplitude (frequency) that decreases (increases) as the energy decreases. The spectra are normalized such that the SSM spectrum integrates to one.

FIG. 2. The ratio $\Phi^{\mu}_{pp}/\Phi^{SSM}_{pp}$ predicted by the four *good* solutions in *pp* energy range. Diamonds indicate the best fit predictions and error bars show the range of values allowed at the 90% CL.

FIG. 3. Same as Fig. 2 for *pep* neutrinos.

FIG. 4. The ratio $\Phi^{\mu}_{pep}/\Phi^{SSM}_{pep}$ vs. the ratio $\Phi^{\mu}_{pp}/\Phi^{SSM}_{pp}$ as they are predicted by the three *good* solutions to the SNP with oscillations into active neutrinos. Diamonds indicate the predictions at the best fit parameters. Areas contain the corresponding ranges of parameters allowed at the 90% CL. Oscillations into sterile neutrinos obviously give only the point at the origin.

FIG. 5. Possible outcomes of a combined measurement of Φ^{e}_{pp} and Φ^{μ}_{pp}. The dashed line is the upper bound due to the luminosity constraint, Eq. (11). The shaded band shows the range of predictions allowed by the uncertainties of the SSMs in case of oscillations into active neutrinos. The solid arrows indicate the prediction at the best fit parameters for the four solutions considered. The dashed arrows show the corresponding ranges of parameters allowed at the 90% CL.

FIG. 6. Same as Fig. 5 for *pep* neutrinos.

FIG. 7. The ratio of the ν_e spectrum on Earth in the *pp* energy region ($150 < E < 440$ keV) predicted by the Just-So best fit (a) for active neutrinos over the spectrum of the SSM. The effect of averaging the spectrum predicted by the Just-So best fit solution over an energy window of $\Delta E =$ (b) 10, (c) 20 and (d) 50 keV is also shown.

FIG. 8. The expected time dependence of the *pep* electron neutrino survival probability $\Phi^{e}_{pep}/\Phi^{SSM}_{pep}$ (solid line) as function of the absolute time difference from the perihelion in fraction of year (0.5 is then the aphelion). The dashed line shows instead the signal S_{pep}/S^{SSM}_{pep}, see Eqs. (13) and (15). The oscillation parameters, Δm^2 and θ, are those that give the maximal variation within the 90% confidence region.

FIG. 9. Same as Fig. 4 with the ratio $\Phi^{\mu}_{pep}/\Phi^{SSM}_{pep}$ replaced by the quantity that should be measured by Hellaz S_{pep}/S^{SSM}_{pep}. In this case, oscillations into sterile neutrinos give a non-zero value for S_{pep}/S^{SSM}_{pep} and the range of values allowed at the 90% CL by this solution lies along the vertical axis.

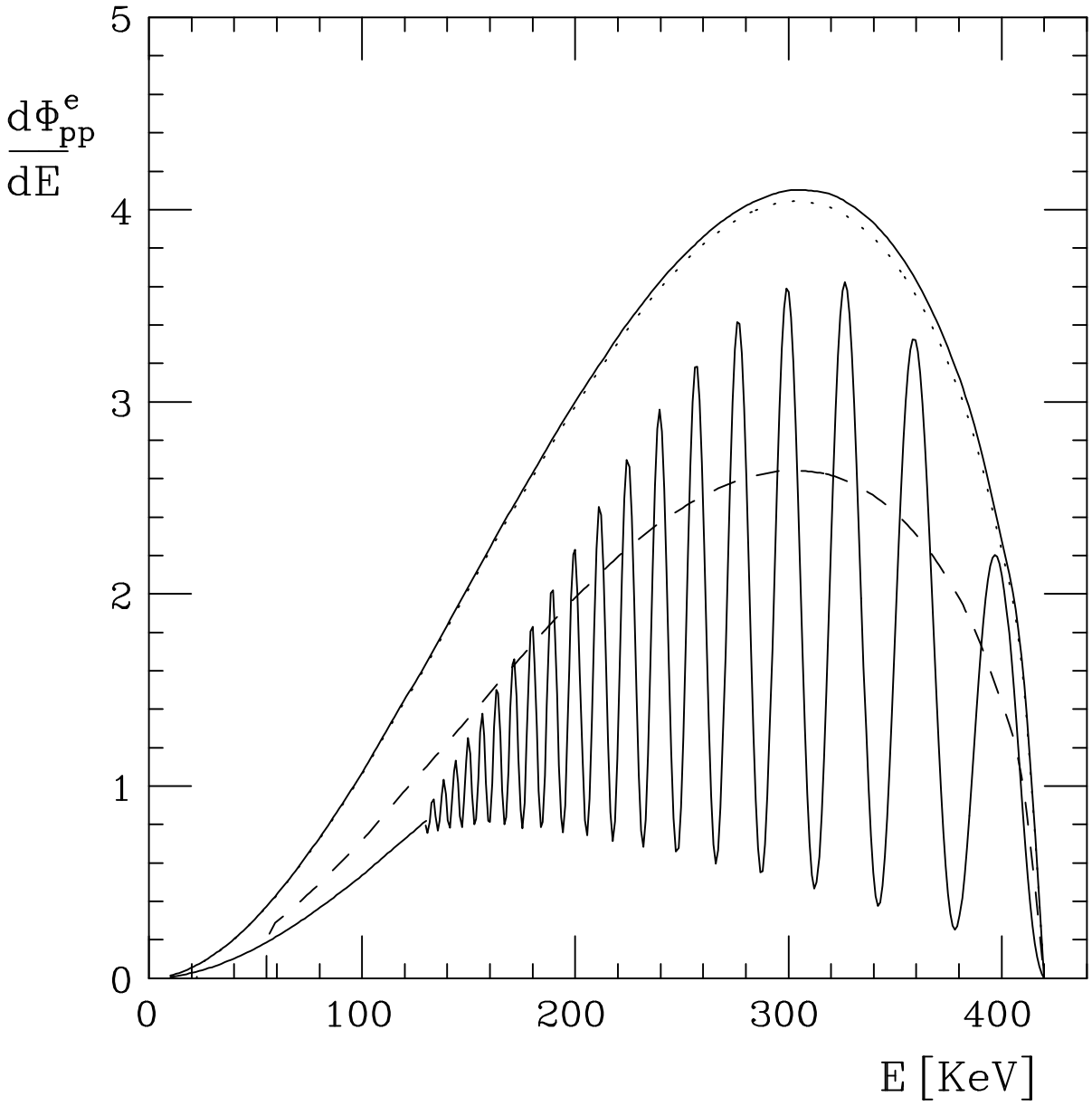

Fig.1

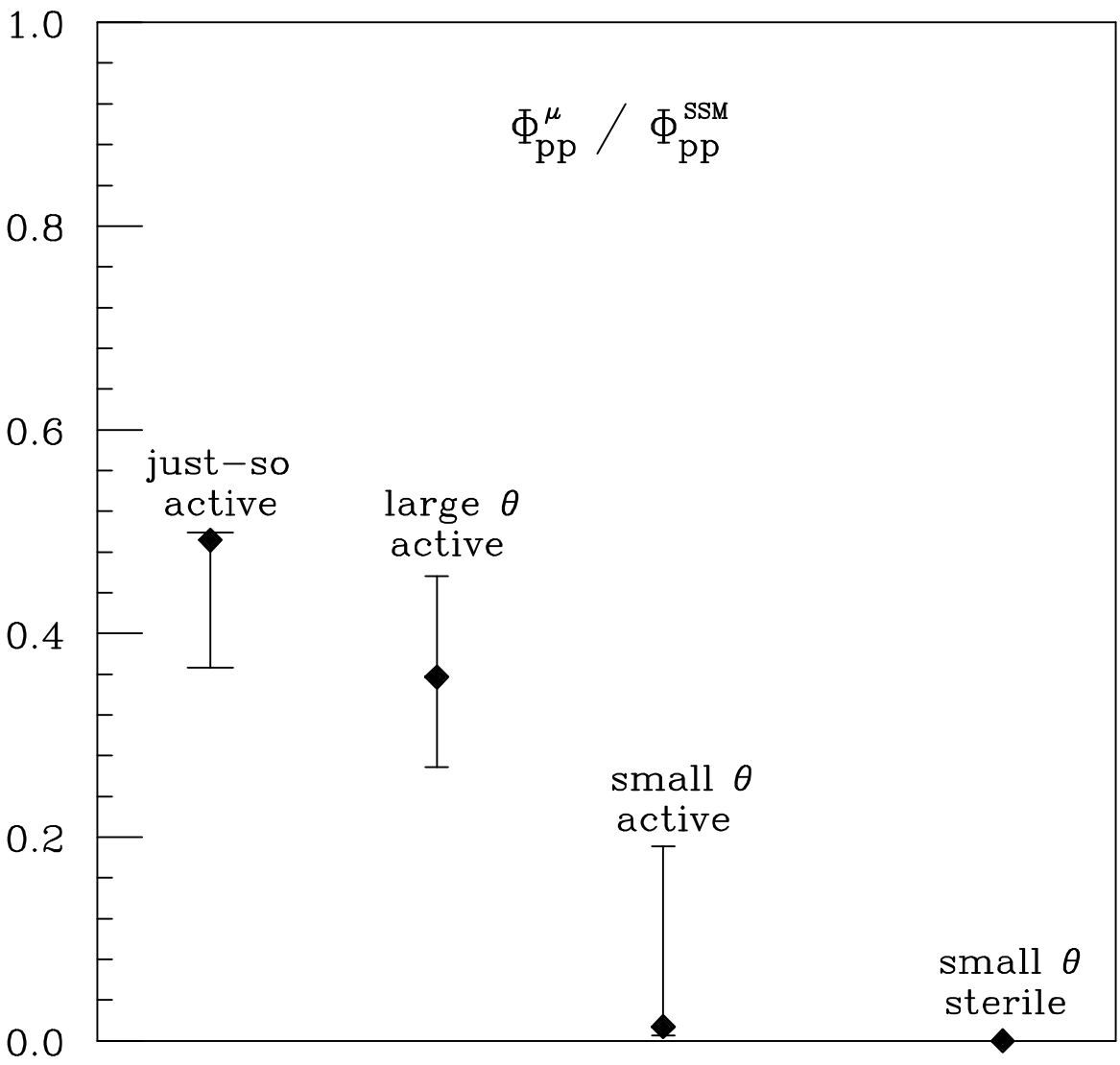
1.0
0.8
0.6
0.4
0.2
0.0
$\Phi_{pp}^{\mu} \ / \ \Phi_{pp}^{SSM}$
just−so
active
large θ
active
small θ
active
small θ
sterile

Fig.2

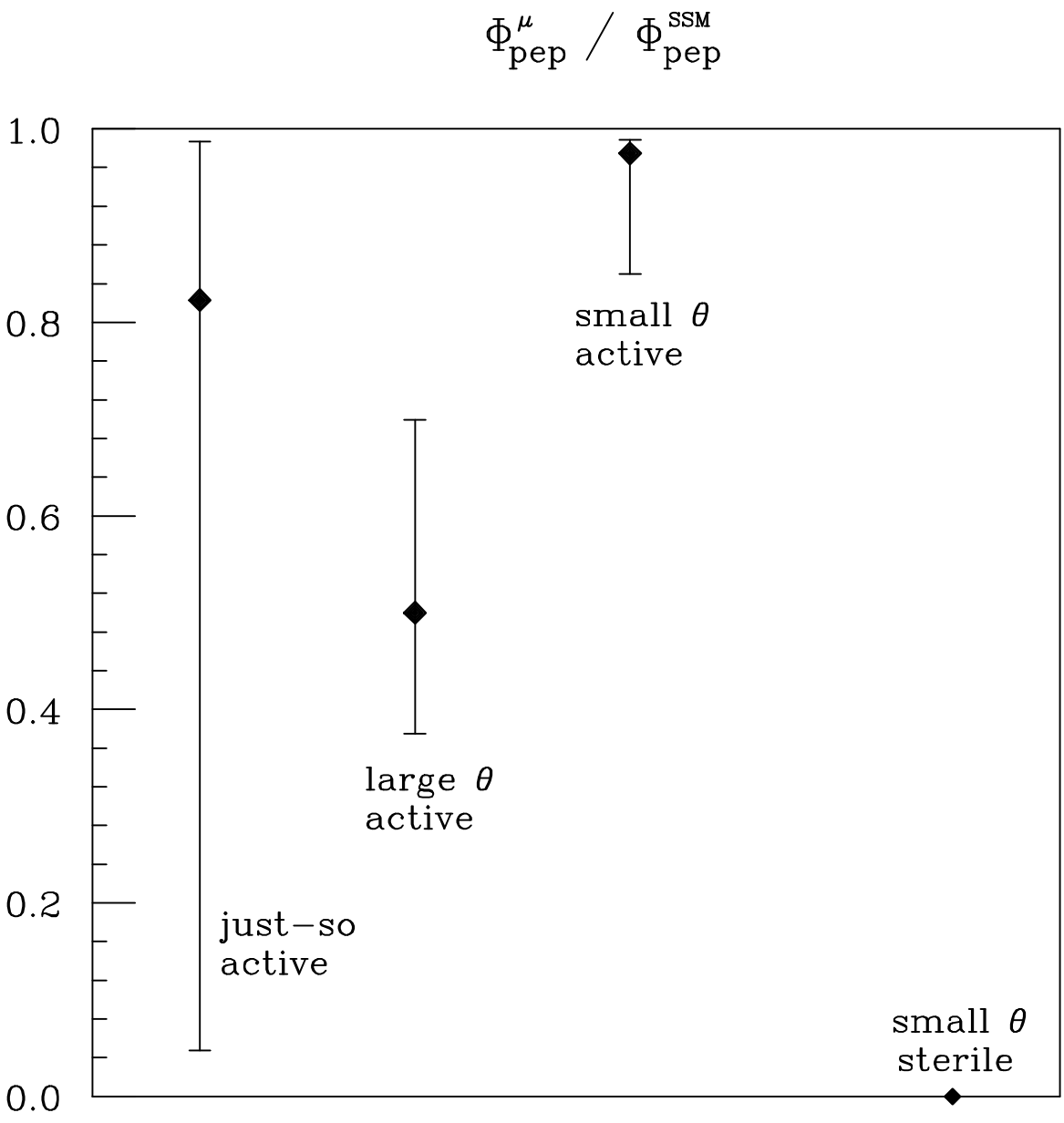
$\Phi^{\mu}_{pep} \;/\; \Phi^{SSM}_{pep}$
1.0
0.8
0.6
0.4
0.2
0.0
small θ
active
large θ
active
just−so
active
small θ
sterile

Fig.3

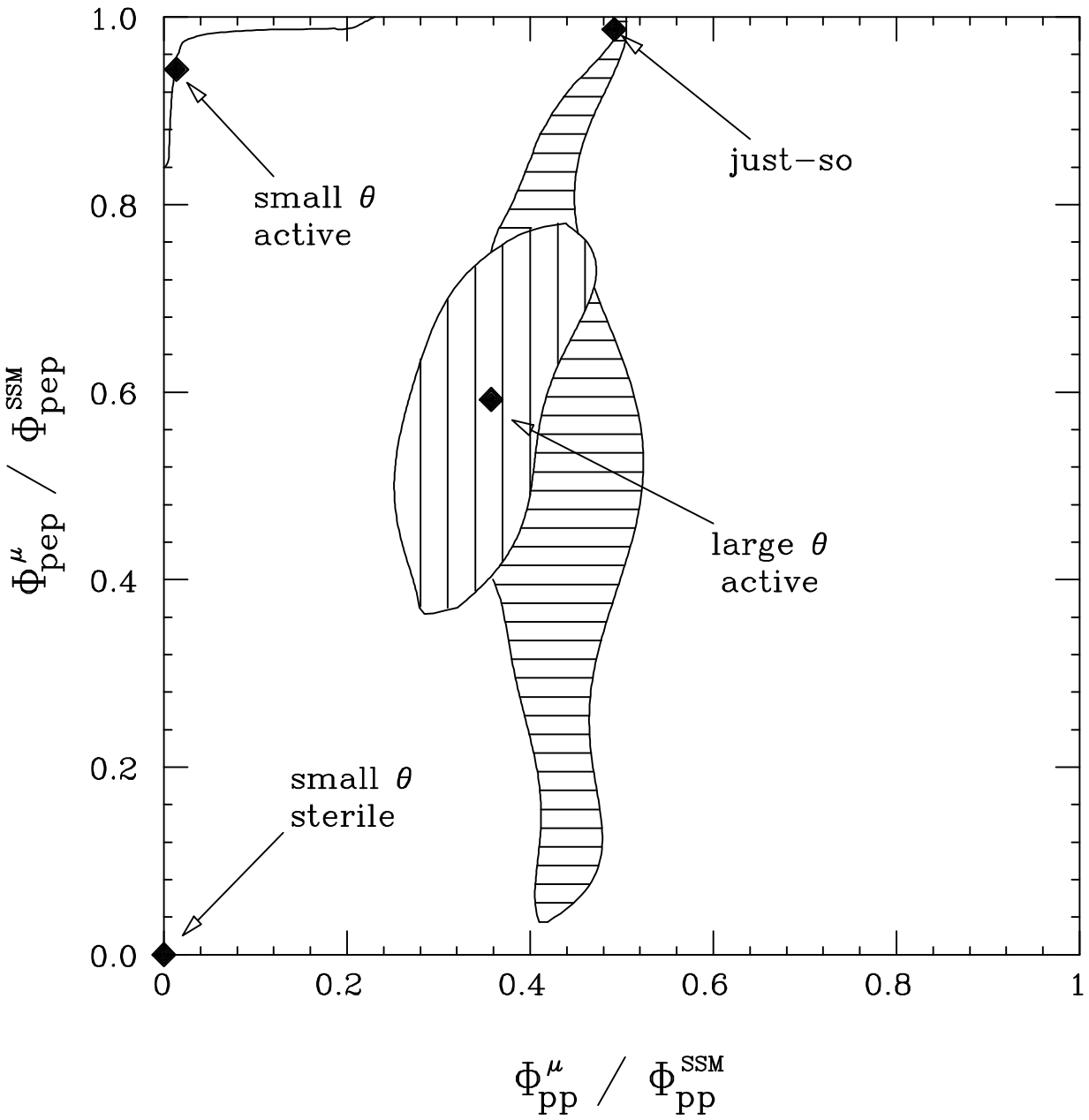
1.0
0.8
0.6
0.4
0.2
0.0
0
0.2
0.4
0.6
0.8
1
small θ
active
just−so
large θ
active
small θ
sterile
$\Phi^{\mu}_{pep} \;/\; \Phi^{SSM}_{pep}$
$\Phi^{\mu}_{pp} \;/\; \Phi^{SSM}_{pp}$

Fig.4

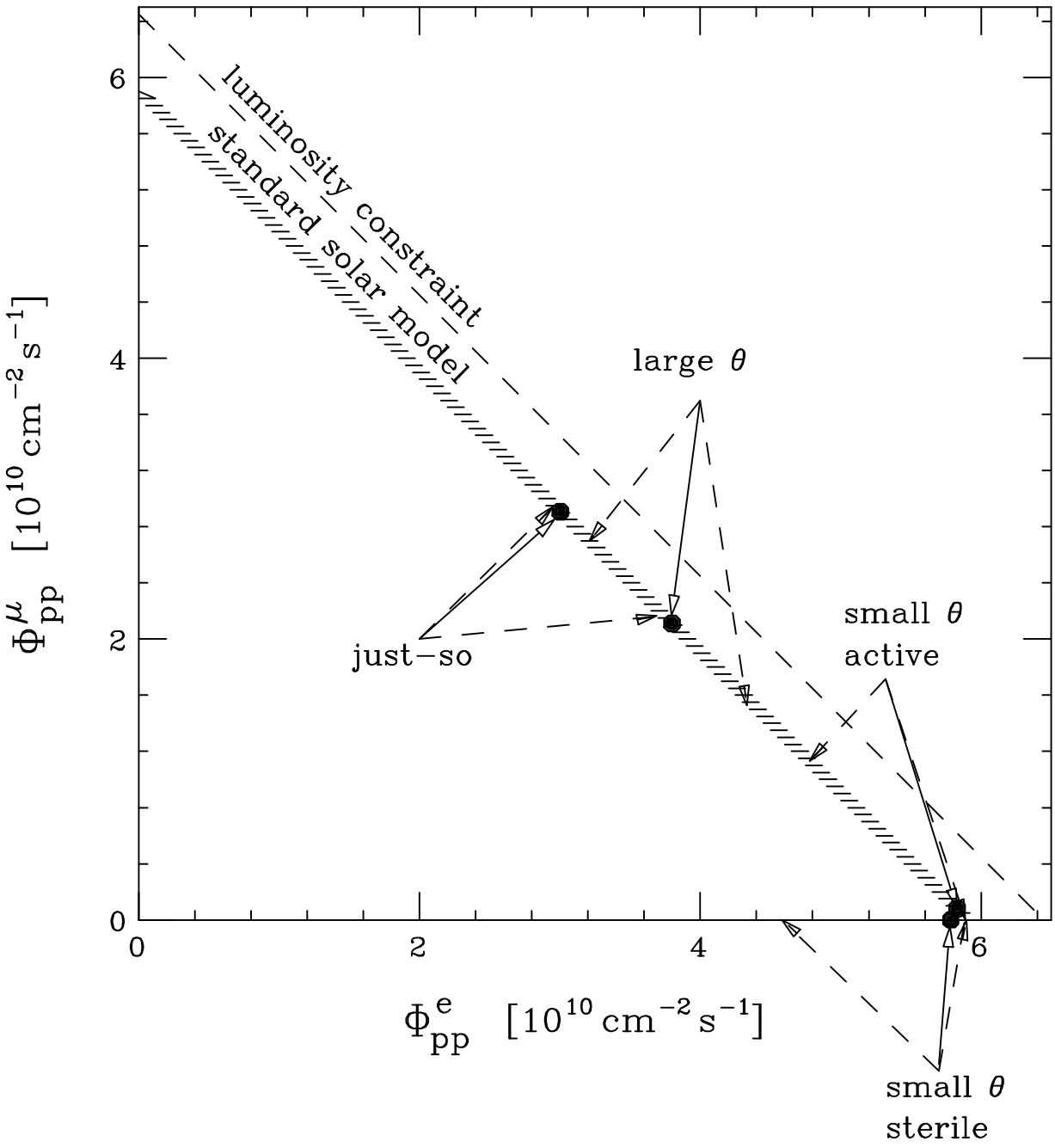
luminosity constraint
standard solar model
large θ
small θ
active
small θ
sterile
just−so
Φ^{μ}_{pp} [10^{10} cm^{-2} s^{-1}]
Φ^{e}_{pp} [10^{10} cm^{-2} s^{-1}]
0
2
4
6

Fig.5

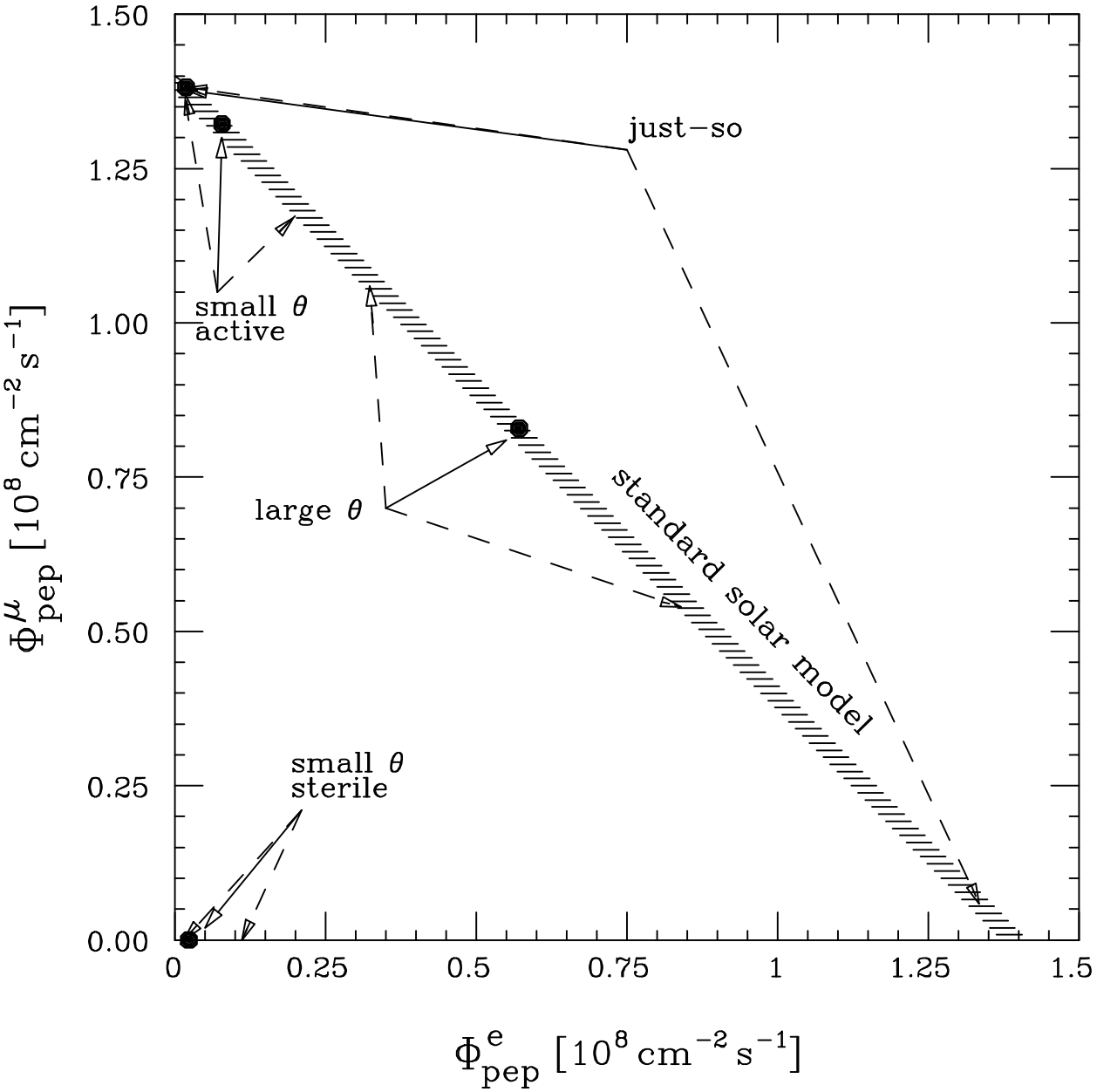
1.50
1.25
1.00
0.75
0.50
0.25
0.00
0
0.25
0.5
0.75
1
1.25
1.5
just−so
small θ
active
large θ
standard solar model
small θ
sterile
Φ^{μ}_{pep} [10^8 cm^{-2} s^{-1}]
Φ^{e}_{pep} [10^8 cm^{-2} s^{-1}]

Fig.6

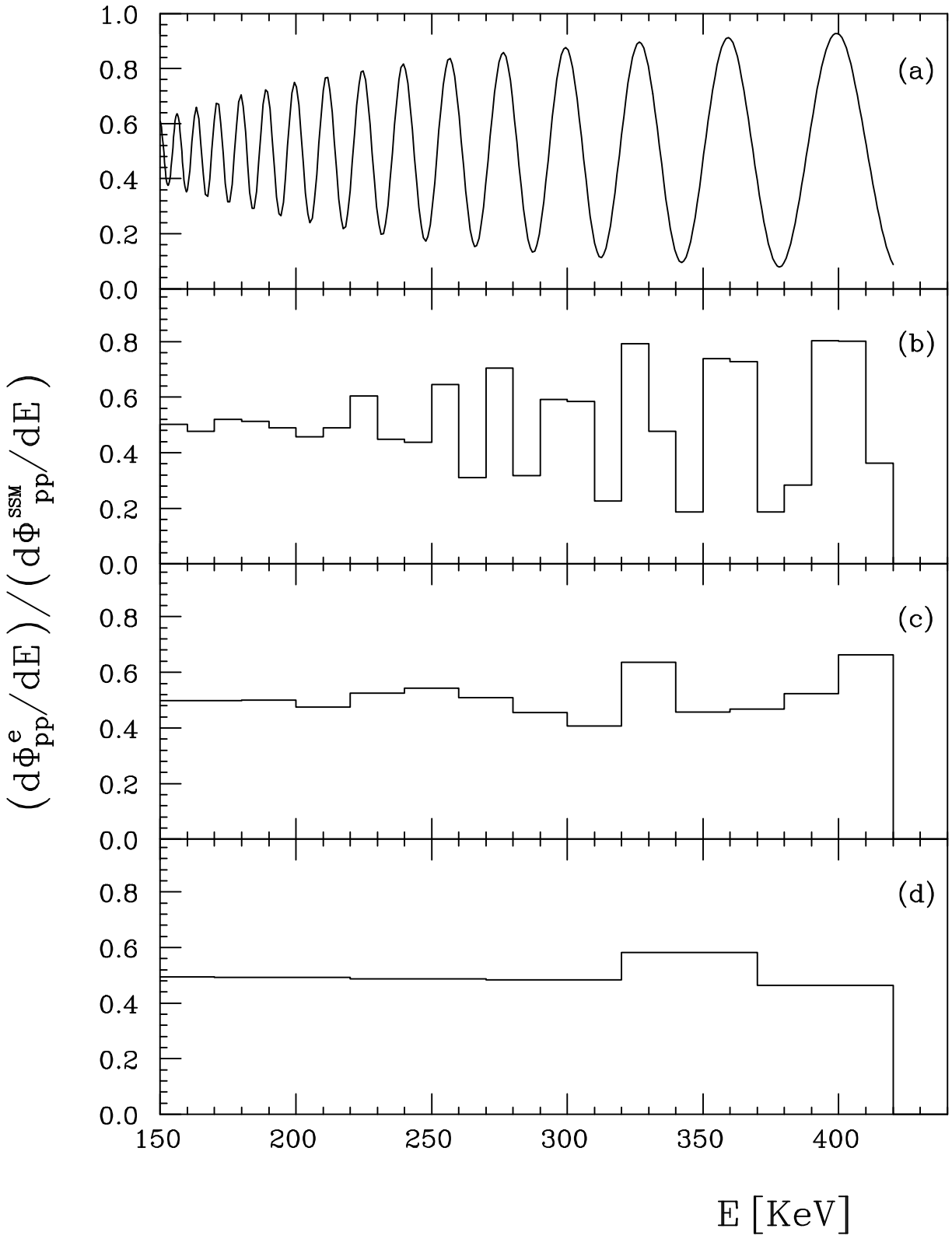
1.0
0.8
0.6
0.4
0.2
0.0
(a)
(b)
(c)
(d)
150
200
250
300
350
400
E [KeV]
$\left(d\Phi^{e}_{pp}/dE\right)/\left(d\Phi^{SSM}_{pp}/dE\right)$

Fig.7

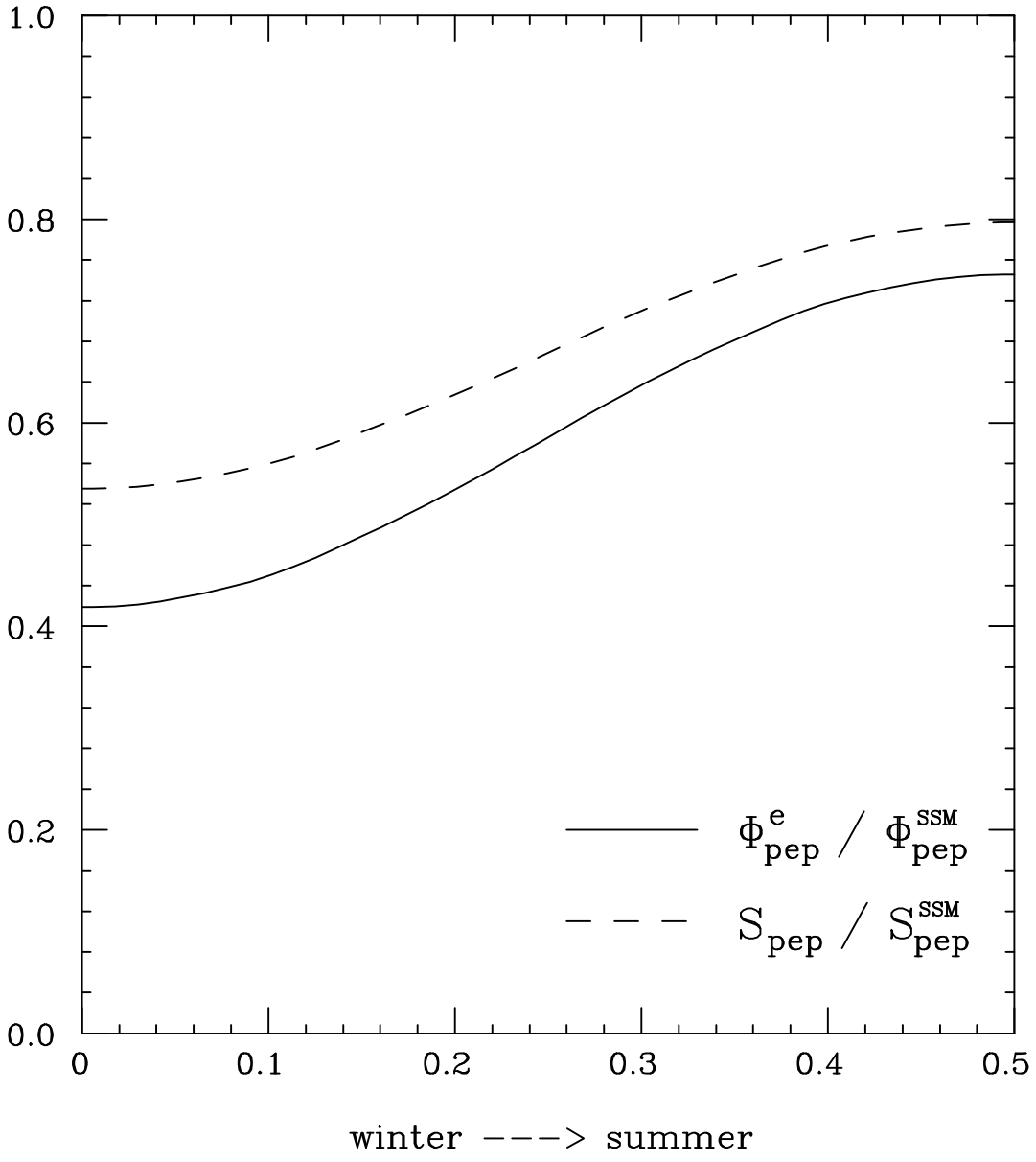
1.0
0.8
0.6
0.4
0.2
0.0
0
0.1
0.2
0.3
0.4
0.5
$\Phi^{e}_{pep} / \Phi^{SSM}_{pep}$
S_{pep} / S^{SSM}_{pep}
winter ---> summer

Fig.8

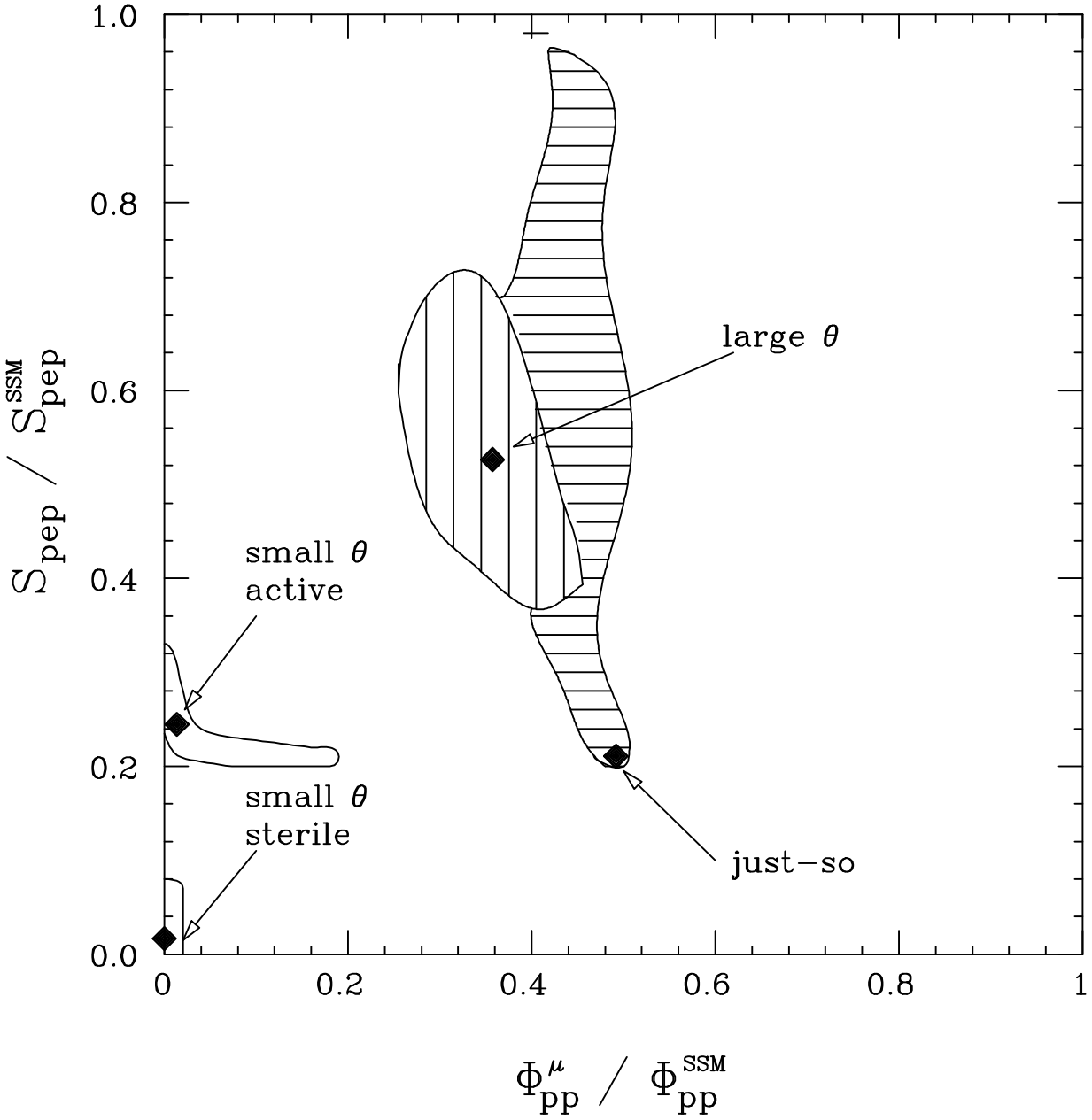
1.0
0.8
0.6
0.4
0.2
0.0
0
0.2
0.4
0.6
0.8
1
large θ
small θ
active
small θ
sterile
just−so
$\Phi^{\mu}_{pp} / \Phi^{SSM}_{pp}$
$\Phi^{\mu}_{pep} / \Phi^{SSM}_{pep}$

Fig.9